Study of 3-prong hadronic τ decays with charged kaons

S. J. Richichi, H. Severini, P. Skubic, and A. Undrus
University of Oklahoma, Norman, Oklahoma 73019

M. Bishai, S. Chen, J. Fast, J. W. Hinson, N. Menon, D. H. Miller, E. I. Shibata, and I. P. J. Shipsey
Purdue University, West Lafayette, Indiana 47907

S. Glenn, Y. Kwon,* A. L. Lyon, S. Roberts, and E. H. Thorndike
University of Rochester, Rochester, New York 14627

C. P. Jessop, K. Lingel, H. Marsiske, M. L. Perl, V. Savinov, D. Ugolini, and X. Zhou
Stanford Linear Accelerator Center, Stanford University, Stanford, California 94309

T. E. Coan, V. Fadeyev, I. Korolkov, Y. Maravin, I. Narsky, R. Stroynowski, and J. Ye
Southern Methodist University, Dallas, Texas 75275

M. Artuso, E. Dambasuren, S. Kopp, G. C. Moneti, R. Mountain, S. Schuh, T. Skwarnicki, S. Stone, A. Titov,
G. Viehhauser, and J. C. Wang
Syracuse University, Syracuse, New York 13244

J. Bartelt, S. E. Csorna, K. W. McLean, S. Marka, and Z. Xu
Vanderbilt University, Nashville, Tennessee 37235

R. Godang, K. Kinoshita, I. C. Lai, P. Pomianowski, and S. Schrenk
Virginia Polytechnic Institute and State University, Blacksburg, Virginia 24061

G. Bonvicini, D. Cinabro, R. Greene, L. P. Perera, and G. J. Zhou
Wayne State University, Detroit, Michigan 48202

S. Chan, G. Eigen, E. Lipeles, J. S. Miller, M. Schmidtler, A. Shapiro, W. M. Sun, J. Urheim, A. J. Weinstein,
and F. Würthwein
California Institute of Technology, Pasadena, California 91125

D. W. Bliss, D. E. Jaffe, G. Masek, H. P. Paar, E. M. Potter, S. Prell, and V. Sharma
University of California, San Diego, La Jolla, California 92093

D. M. Asner, J. Gronberg, T. S. Hill, D. J. Lange, R. J. Morrison, H. N. Nelson, T. K. Nelson, and D. Roberts
University of California, Santa Barbara, California 93106

B. H. Behrens, W. T. Ford, A. Gritsan, H. Krieg, J. Roy, and J. G. Smith
University of Colorado, Boulder, Colorado 80309-0390

J. P. Alexander, R. Baker, C. Bebek, B. E. Berger, K. Berkelman, V. Boisvert, D. G. Cassel, D. S. Crowcroft, M. Dickson,
S. von Dombrowski, P. S. Drell, K. M. Ecklund, R. Ehrlich, A. D. Foland, P. Gaidarev, R. S. Galik, L. Gibbons,
B. Gittelman, S. W. Gray, D. L. Hartill, B. K. Heltsley, P. I. Hopman, J. Kandaswamy, D. L. Kreinick, T. Lee, Y. Liu,
N. B. Mistry, C. R. Ng, E. Nordberg, M. Ogg,[†] J. R. Patterson, D. Peterson, D. Riley, A. Soffer, B. Valant-Spaight,
and C. Ward
Cornell University, Ithaca, New York 14853

M. Athanas, P. Avery, C. D. Jones, M. Lohner, S. Patton, C. Prescott, A. I. Rubiera, J. Yelton, and J. Zheng
University of Florida, Gainesville, Florida 32611

G. Brandenburg, R. A. Briere, A. Ershov, Y. S. Gao, D. Y.-J. Kim, R. Wilson, and H. Yamamoto
Harvard University, Cambridge, Massachusetts 02138

T. E. Browder, Y. Li, J. L. Rodriguez, and S. K. Sahu
University of Hawaii at Manoa, Honolulu, Hawaii 96822

T. Bergfeld, B. I. Eisenstein, J. Ernst, G. E. Gladding, G. D. Gollin, R. M. Hans, E. Johnson, I. Karliner, M. A. Marsh, M. Palmer, M. Selen, and J. J. Thaler
University of Illinois, Urbana-Champaign, Illinois 61801

K. W. Edwards
*Carleton University, Ottawa, Ontario, Canada K1S 5B6
and the Institute of Particle Physics, Canada*

A. Bellerive, R. Janicek, and P. M. Patel
*McGill University, Montréal, Québec, Canada H3A 2T8
and the Institute of Particle Physics, Canada*

A. J. Sadoff
Ithaca College, Ithaca, New York 14850

R. Ammar, P. Baringer, A. Bean, D. Besson, D. Coppage, C. Darling, R. Davis, S. Kotov, I. Kravchenko, N. Kwak, and L. Zhou
University of Kansas, Lawrence, Kansas 66045

S. Anderson, Y. Kubota, S. J. Lee, R. Mahapatra, J. J. O'Neill, R. Poling, T. Riehle, and A. Smith
University of Minnesota, Minneapolis, Minnesota 55455

M. S. Alam, S. B. Athar, Z. Ling, A. H. Mahmood, S. Timm, and F. Wappler
State University of New York at Albany, Albany, New York 12222

A. Anastassov, J. E. Duboscq, K. K. Gan, T. Hart, K. Honscheid, H. Kagan, R. Kass, J. Lee, H. Schwarthoff, M. B. Spencer, A. Wolf, and M. M. Zoeller
Ohio State University, Columbus, Ohio 43210

(CLEO Collaboration)

Using a sample of 4.7 fb^{-1} integrated luminosity accumulated with the CLEO-II detector at the Cornell Electron Storage Ring (CESR), we have measured the ratios of the branching fractions $\mathcal{B}(\tau^- \to K^- h^+ \pi^- \nu_\tau)/\mathcal{B}(\tau^- \to h^- h^+ h^- \nu_\tau) = (5.16 \pm 0.20 \pm 0.50) \times 10^{-2}$, $\mathcal{B}(\tau^- \to K^- h^+ \pi^- \pi^0 \nu_\tau)/\mathcal{B}(\tau^- \to h^- h^+ h^- \pi^0 \nu_\tau) = (2.54 \pm 0.44 \pm 0.39) \times 10^{-2}$, $\mathcal{B}(\tau^- \to K^- K^+ \pi^- \nu_\tau)/\mathcal{B}(\tau^- \to h^- h^+ h^- \nu_\tau) = (1.52 \pm 0.14 \pm 0.29) \times 10^{-2}$, and the upper limit $\mathcal{B}(\tau^- \to K^- K^+ \pi^- \pi^0 \nu_\tau)/\mathcal{B}(\tau^- \to h^- h^+ h^- \pi^0 \nu_\tau) < 0.0154$ at 95% C.L. Coupled with additional experimental information, we use our results to extract information on the structure of three-prong tau decays to charged kaons. [S0556-2821(99)03319-6]

PACS number(s): 13.35.Dx

I. INTRODUCTION

Decays of the τ lepton present a unique opportunity to confirm and further probe the standard model. The large mass of the τ lepton makes possible decays into hadrons in an environment where the initial state is simple and well understood [1]. This allows comparison with hadron production at comparable center of mass energies from processes such as pion-nucleon, nucleon-nucleon, and electron-positron collisions. Strange τ decays give us information on $SU(3)_f$ symmetry breaking, and direct measurements of the Cabibbo angle (θ_c). Alternately, the rates for such Cabibbo-suppressed decays (e.g., $\tau \to K \nu_\tau$, $\tau \to K^* \nu_\tau$, and $\tau \to K_1 \nu_\tau$)

can be predicted using corresponding measurements of the Cabibbo favored modes ($\tau \to \pi \nu_\tau$, $\tau \to \rho \nu_\tau$, and $\tau \to a_1 \nu_\tau$). For the case of vector coupling, the theoretically expected ratio of the branching ratios $\mathcal{B}(\tau \to K^* \nu_\tau)/\mathcal{B}(\tau \to \rho \nu_\tau)$ [2] can be written following the approach of the Das-Mathur-Okubo sum rules [3] as $f(m_{K*}, m_\rho, m_\tau) \tan^2 \theta_c g_{K*}^2 / g_\rho^2$, where f is a factor that incorporates the phase space available for decays into ρ and K^*, θ_c is the Cabibbo angle, and the factors g_{K*} and g_ρ reflect the coupling strengths of the K^* and ρ to the vector current. In the limit of exact SU(3) symmetry, there is no differentiation between the K^* and the ρ, so $g_{K*} = g_\rho$. In the more realistic case of broken symmetry, however, the couplings g are directly proportional to mass. In this approximation, using $\sin \theta_c = 0.221$ [4], the ratio of rates equals 0.068. There are many experimental results for $\tau \to K^* \nu_\tau$ (where the charged K^* is observed through the very clean decay chain $K^* \to K_S^0 \pi$; $K_S^0 \to \pi^+ \pi^-$) which are

---

*Permanent address: Yonsei University, Seoul 120-749, Korea.
†Permanent address: University of Texas, Austin, TX 78712.

in agreement with this prediction [4].

We expect similar relationships to hold for the coupling of the tau to the axial vector K_1 resonance relative to the a_1 resonance. Unfortunately, $\tau \rightarrow K_1 \nu_\tau$ is not as well studied as $\tau \rightarrow K^* \nu_\tau$, in part due to the fact that the K_1 decay most often leads to multiprong events that include charged kaons. Whereas the K^* can be unambiguously identified through its decay $K^* \rightarrow K_S^0 \pi$, a measurement of charged kaons requires good K/π particle identification in order to separate kaons from the substantially more numerous pions. Moreover, theoretical understanding of charged kaon production in tau decay is hampered by uncertainties in the production mechanism; there is a wide range of predictions for the mass spectrum [expected to be dominated by $K_1(1270)$ and $K_1(1400)$], the $K^* \pi / K \rho$ ratio (in $K \pi \pi$), and the helicity amplitudes for τ decays to kaons.

In recent years the large data samples accumulated at CLEO and CERN e^+e^- collider LEP have allowed much-improved measurements of inclusive decays of tau leptons to charged kaons, complementing similar measurements of inclusive decays of tau leptons to neutral kaons. In this analysis we measure the ratio of branching fractions of $\tau^- \rightarrow K^- h^+ \pi^- (\pi^0) \nu_\tau$ and $\tau^- \rightarrow K^- K^+ \pi^- (\pi^0) \nu_\tau$ relative to $\tau^- \rightarrow h^- h^+ h^- (\pi^0) \nu_\tau$, where $h^\pm$ can be either a charged pion or kaon.[1] The decay $\tau \rightarrow K^- \pi^+ \pi^- (\pi^0) \nu_\tau$ proceeding through the $K^- K^0 (\pi^0) \nu_\tau$ intermediate state has been measured in Ref. [5]; in our analysis, these are considered background since we are interested in studying tau decays directly into 3 or 4 mesons that include charged kaons.

II. DATA SAMPLE AND EVENT SELECTION

Our data sample contains approximately 4.3 million τ pairs produced in e^+e^- collisions, corresponding to an integrated luminosity of 4.7 fb^{-1}. The data were collected with the CLEO-II detector [6] at the Cornell Electron Storage Ring operating at a center-of-mass energy of approximately 10.58 GeV.

The CLEO II detector is a general purpose solenoidal magnet spectrometer and calorimeter. The detector was designed for efficient triggering and reconstruction of two-photon, tau-pair, and hadronic events. Measurements of charged particle momenta are made with three nested coaxial drift chambers consisting of 6, 10, and 51 layers, respectively. These chambers fill the volume from $r = 3$ cm to $r = 1$ m, with r the radial coordinate relative to the beam ($\hat{z}$) axis. This system is very efficient ($\epsilon \geq 98\%$) for detecting tracks that have transverse momenta (p_T) relative to the beam axis greater than 200 MeV/c, and that are contained within the good fiducial volume of the drift chamber ($|\cos \theta| < 0.94$, with θ defined as the polar angle relative to the beam axis). The charged particle detection efficiency in the fiducial volume decreases to approximately 90% at $p_T \sim 100$ MeV/c. For $p_T < 100$ MeV/c, the efficiency decreases roughly linearly to zero at a threshold of p_T

≈ 30 MeV/c. This system achieves a momentum resolution of $(\delta p / p)^2 = (0.0015p)^2 + (0.005)^2$ (p is the momentum, measured in GeV/c). Pulse height measurements in the main drift chamber provide specific ionization (dE/dx) resolution of 5.5% for Bhabha events, giving good K/π separation for tracks with momenta up to 700 MeV/c and separation nearly 2σ in the relativistic rise region above 2 GeV/c. Outside the central tracking chambers are plastic scintillation counters, which are used as a fast element in the trigger system and also provide particle identification information from time-of-flight measurements.

Beyond the time-of-flight system is the electromagnetic calorimeter, consisting of 7800 thallium-doped CsI crystals. The central ''barrel'' region of the calorimeter covers about 75% of the solid angle and has an energy resolution which is empirically found to follow

$$\frac{\sigma_E}{E}(\%) = \frac{0.35}{E^{0.75}} + 1.9 - 0.1E, \tag{1}$$

E is the shower energy in GeV. This parametrization includes effects such as noise, and translates to an energy resolution of about 4% at 100 MeV and 1.2% at 5 GeV. Two end-cap regions of the crystal calorimeter extend solid angle coverage to about 95% of 4π, although energy resolution is not as good as that of the barrel region. The tracking system, time of flight counters, and calorimeter are all contained within a superconducting coil operated at 1.5 T. Flux return and tracking chambers used for muon detection are located immediately outside the coil and in the two end-cap regions.

We select $e^+e^- \rightarrow \tau^+\tau^-$ events having a ''1 vs 3'' topology in which one τ lepton decays into one charged particle (plus a possible π^0), and the other τ lepton decays into three charged hadrons (plus possible π^0). An event is separated into two hemispheres based on the measured event thrust axis.[2] At CLEO energies, the decay products of the τ leptons are strongly boosted so that the daughters of the τ^+ and τ^- appear in opposite hemispheres. Loose cuts on ionization measured in the drift chamber, energy deposited in the calorimeter and the maximum penetration depth into the muon detector system are applied to charged tracks in the signal (three-prong) hemisphere to reject leptons. Backgrounds from τ and hadronic events with K_S^0 are suppressed by requirements on the impact parameters of charged tracks. To reduce the background from two-photon collisions ($e^+e^- \rightarrow e^+e^- \gamma\gamma$ with $\gamma\gamma \rightarrow$ hadrons or $\gamma\gamma \rightarrow l^+l^-$), cuts on visible energy (E_{vis}) and total event transverse momentum (P_t) are applied: 2.5 GeV $< E_{\text{vis}} < 10$ GeV and $P_t > 0.3$ GeV/c. We also require the invariant mass of the tracks and showers in the three-prong hemisphere, calculated under the $\pi^- \pi^+ \pi^-$ hypothesis, to be less than 1.7 GeV/c.

Events are accepted for which the tag hemisphere (one-prong side) is consistent with one of the following four de-

---

[1]Charge conjugate modes are implied throughout the paper.

---

[2]The thrust axis of an event is chosen so that the sum of longitudinal (relative to this axis) momenta of all charged tracks has a maximum value.

cays: $\tau^+ \to e^+ \nu_e \bar{\nu}_\tau$, $\tau^+ \to \mu^+ \nu_\mu \bar{\nu}_\tau$, $\tau^+ \to \pi^+ \bar{\nu}_\tau$, or $\tau^+ \to \rho^+ \bar{\nu}_\tau$. The tag decays are identified using dE/dx and information from the time-of-flight system, the muon system and the crystal calorimeter. For the ρ tag, the daughter π^0 is reconstructed and the invariant mass of the ρ candidate is required to be close to the nominal value.

In this measurement, we determine the signal event yield based on a statistical analysis of the charged tracks' dE/dx information. For the $\tau^- \to K^- h^+ \pi^- (\pi^0) \nu_\tau$ analysis, we determine the kaon and pion yields, using the two same-sign tracks from the three-prong hemisphere. For the $\tau^- \to K^- K^+ \pi^- (\pi^0) \nu_\tau$ mode, only the track having sign opposite to its parent τ is considered as a candidate kaon. Note that we implicitly assume that all signal kaons originating from τ decays in our selected 1 vs 3 samples come from one of the decay modes $\tau^- \to K^- \pi^+ \pi^- \nu_\tau$, $\tau^- \to K^- K^+ \pi^- \nu_\tau$, $\tau^- \to K^- \pi^+ \pi^- \pi^0 \nu_\tau$, or $\tau^- \to K^- K^+ \pi^- \pi^0 \nu_\tau$. The decays $\tau^- \to \pi^- K^+ \pi^- \nu_\tau$ and $\tau^- \to K^- \pi^+ K^- \nu_\tau$ are extremely small in the standard model and have not been experimentally observed, and the decay rate for $\tau^- \to K^- K^+ K^- \nu_\tau$ is expected to be $\sim 1\%$ relative to that for $\tau^- \to K^- \pi^+ \pi^- \nu_\tau$ due to the limited phase space and the low probability of $(s \bar{s})$ popping.

Candidate events with and without π^0's are distinguished by the characteristics of showers in the electromagnetic calorimeter. A ''photon'' candidate is defined as a shower in the barrel region of the electromagnetic calorimeter with energy above 40 MeV and having an energy deposition pattern consistent with true photons. It must be separated from the closest charged track by at least 30 cm (20 cm for photons used in π^0 reconstruction). $\tau^- \to K^- h^+ \pi^- \nu_\tau$ and $\tau^- \to K^- K^+ \pi^- \nu_\tau$ candidates are defined as those events having zero photons with energy above 100 MeV in the three-prong hemisphere. For the $\tau^- \to K^- h^+ \pi^- \pi^0 \nu_\tau$ and $\tau^- \to K^- K^+ \pi^- \pi^0 \nu_\tau$ decay modes there must be at least two photons in the signal hemisphere, but no more than two photon candidates having a shower energy above 100 MeV. The two most energetic photons in this hemisphere are then paired to form π^0 candidates.

III. SIGNAL EXTRACTION PROCEDURE

To find the number of events with kaons, we use specific ionization information from the central drift chamber. For each track we calculate the parameter δ_K, defined as the deviation of the measured energy loss relative to that expected for true kaons in units of the measured dE/dx resolution. For true kaons, this variable is distributed as a unit Gaussian centered at 0. For pion tracks, δ_k also has a Gaussian-like shape but with the mean shifted from zero in a momentum-dependent manner. In this analysis we concentrate on those tracks having momentum $p > 1.5$ GeV/c. Although the K/π separation is better at low momenta, we focus on this high momentum region because the separation varies only slowly through this regime and the systematics of signal extraction are therefore more tractable. These tracks generally have the highest momenta of the tracks in the three-prong hemisphere and are well separated spatially from
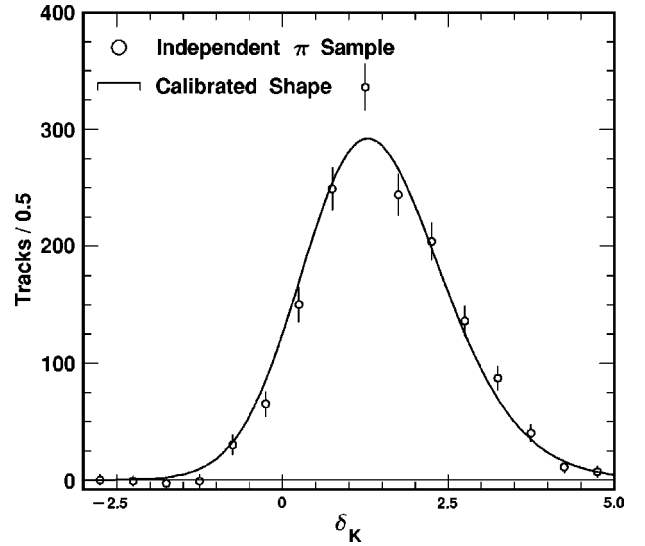

FIG. 1. Distribution for independent pion sample (from D^0 decays) with Johnson distribution for pions obtained from the $K_S^0 \to \pi^+ \pi^-$ calibration sample overlaid. The data on this plot correspond to the bin: $1.9 < p < 2.1$ GeV/c, $20 < N_{hit} < 50$.

the lower momentum tracks. Non-τ background as well as the pion background relative to the desired kaon signal in real τ decays is also smaller at high momenta.

The number of kaon and pion tracks in the three-prong hemisphere is found statistically by fitting the δ_k distribution for charged tracks in the three-prong hemisphere to the sum of the pion and kaon δ_k shapes. Since the K-π separation is modest, it is critical that the shape of the δ_k distribution for pions is well understood. $K_s^0 \to \pi^- \pi^+$ decays provide a very clean sample of true pions from which this distribution can be determined from data. For the pion and kaon shapes, we use a Johnson distribution [7,8] with mean shifted from zero, and a unit Gaussian[3] centered at zero, respectively. The quality of calibration was investigated by various methods such as cross checks on independent data samples which is further described in Sec. VI. In Fig. 1, the shape obtained for pions from the calibration sample is overlaid with an independent sample of pions from D^0 decays showing good agreement. The sample depicted contains tracks with $1.9 < p < 2.1$ GeV/c and $N_{hit} > 20$.

Requirements on the minimum number of hits used in the dE/dx calculation (>20, out of a maximum of 49) and the polar angle of the candidate kaon track ($|\cos \theta| < 0.8$, where θ is the polar angle of the track relative to the positron beam direction) ensure that the track is contained in the good fiducial volume of the drift chamber and that the dE/dx information for the track is of high quality. Since the K/π separation depends on the number of hits (N_{hit}), as well as momentum (p), we perform separate δ_k fits for 36 different bins in the two parameter (N_{hit}, p) space. The kaon and pion

---

[3]The difference in kaon yields obtained using a Johnson distribution rather than a unit Gaussian to represent the kaon δ_k distribution is typically less than 1%.
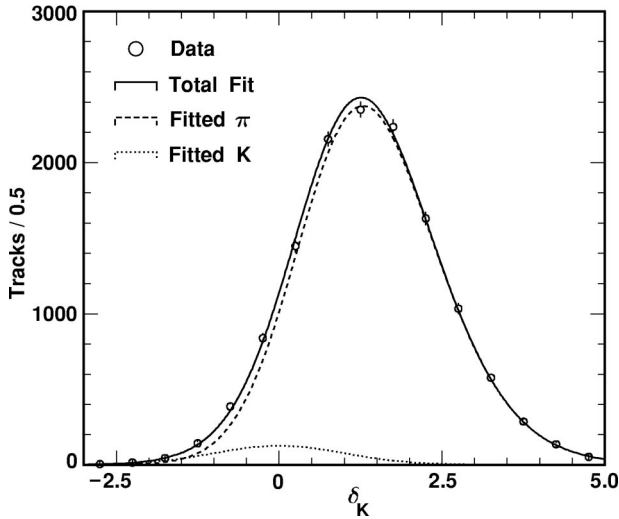
FIG. 2. Fit to δ_k distribution for charged tracks in the three-prong hemisphere of candidate $\tau\tau$ events, with the fitted kaon and pion curves overlaid. The confidence level of the fit is 92%; if the kaon contribution is not included, the C.L. is less than 10^{-3}. The data on this plot correspond to one bin: $1.9 < p < 2.1$ GeV/c, $20 < N_{\text{hit}} < 50$.

FIG. 3. Reconstructed (a) kaon and (b) pion momentum spectra for $\tau \to K h \pi \nu_\tau$ candidates. Solid squares are data points and histogram is the MC shape.

IV. BACKGROUND

There are two primary sources of background: continuum hadronic events ($e^+e^- \to q\bar{q} \to hadrons$) and nonsignal τ decays ("τ feed across"). We estimate hadronic background from a continuum hadronic Monte Carlo sample (using the JETSET v7.3 [9] event generator and GEANT [10] detector simulation code). The kaon and pion momentum spectra resulting from $q\bar{q}$ events that satisfy our selection criteria are found from this Monte Carlo sample and subtracted from the data K/π spectra prior to fitting for the $\tau \to KX$ and $\tau \to \pi X$ yields. The level of hadronic background is shown in Table I.

τ decay modes containing K_S^0 mesons are considered feed-across background, because the major source of τ background to $\tau^- \to K^- h^+ \pi^- (\pi^0) \nu_\tau$ is found to be $\tau^- \to K^- K^0 (\pi^0) \nu_\tau$ decays, in which $K_S^0 \to \pi^+ \pi^-$. There is also contamination of modes without π^0's from modes with π^0's, and vice versa, which we also determine from Monte Carlo simulations, using our measured branching fractions as inputs. Three prong decays with kaons and more than one π^0 are severely phase space suppressed and are neglected in this analysis. The approximate level of τ background is also given in Table I.

yields for each momentum bin above our minimum momentum of 1.5 GeV/c are extracted knowing the pion (and kaon) δ_k shapes appropriate for each N_{hit} interval over a specified momentum range. An example of a δ_k fit, showing the kaon and pion components, is displayed in Fig. 2. The $K:\pi$ mixture in this example is typical of the $\tau^- \to K^- h^+ \pi^- \nu_\tau$ analysis (of order 1:20) and is prepared using all tracks with momenta 1.9 GeV/$c < p < 2.1$ GeV/c and $N_{\text{hit}} > 20$. Note that the data in this plot correspond to the same (N_{hit}, p) bin as the independent pion sample shown in Fig. 1. The shape of the Johnson distribution used for fitting is also identical to that shown in Fig. 1.

To determine the total number of $\tau \to KX$ events, we must extrapolate from our measured yields in the region $p > 1.5$ GeV/c to the lower track momentum region. This is done by fitting the measured kaon and pion momentum spectra to the spectra expected from Monte Carlo (MC) simulations in the $p > 1.5$ GeV/c region, and integrating over the full momentum range. Uncertainties in this MC model are included in our systematic error.

The reconstructed momentum spectrum for the $\tau^- \to K^- h^+ \pi^- \nu_\tau$ analysis is shown in Fig. 3, with the fit overlaid. For decay modes with π^0 mesons, δ_k distributions are made and fitted separately for cases in which the two-photon invariant mass falls in the π^0 signal and sideband regions. The signal region is taken to be $-4 < S_{\gamma\gamma} < 3$, and the sidebands defined as $-18 < S_{\gamma\gamma} < -10$ and $7 < S_{\gamma\gamma} < 17$, where $S_{\gamma\gamma}$ is the number of standard deviations from the π^0 mass. Subtracting the K/π yields from the π^0 sidebands, the K/π signals associated with true π^0 production are determined, and the $\tau^- \to K^- h^+ \pi^- \pi^0 \nu_\tau$ yield is extracted. In Table I we summarize the total yields and backgrounds for all four samples.

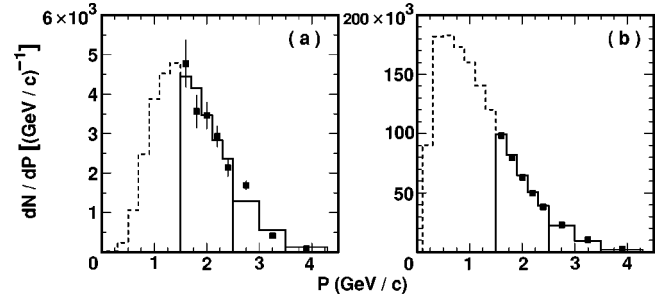## V. NUMERICAL RESULTS

We determine the ratio of branching fractions relative to the normalizing modes directly from the fitted number of kaon and pion tracks in the 1 vs 3 sample. For the $\tau^- \to K^- h^+ \pi^- \nu_\tau$ and $\tau^- \to K^- h^+ \pi^- \pi^0 \nu_\tau$ decay modes, each event contributes two same-sign tracks to the analyzed sample of tracks, one of which is a kaon and one a pion. By contrast, each $\tau^- \to \pi^- \pi^+ \pi^- \nu_\tau$ event contributes 2 pions. Straightforward algebra can be used to find a simple expression for the desired ratio of branching fractions, as outlined in the Appendix. Using this calculation we obtain the results for the ratios (R) of branching fractions shown in Table II. The first error shown is statistical and the second is systematic.

VI. SYSTEMATIC ERRORS

The breakdown of systematic errors for each decay mode is given in Table III. The dominant systematic errors arise

TABLE I. Kaon and pion yields in our 1 vs 3 samples and estimates of background levels. Errors are statistical only. In each pair of numbers in the table the first number pertains to kaons and the second to pions. The τ feed-across background is included in the K/π yields while the hadronic background has already been subtracted.

Hadronic final state	Number of K/π reconstructed	Hadronic background, %	τ feed-across, %
$Kh\pi/\pi\pi\pi$	$7903\pm302/294780\pm1184$	3.1/0.5	9.1/11.2
$Kh\pi\pi^0/\pi\pi\pi\pi^0$	$719\pm123/55140\pm680$	4.9/0.8	9.8/4.5
$KK\pi/\pi\pi\pi$	$2305\pm211/149599\pm761$	5.1/0.4	7.0/14.5
$KK\pi\pi^0/\pi\pi\pi\pi^0$	$158\pm89/26915\pm457$	6.4/0.7	0/7.2

from the uncertainty in the fit procedure used to determine the number of kaons and pions in the 1 vs 3 sample and from the choice of decay models in Monte Carlo simulation. The former error is estimated by performing cross checks on independent mixtures of kaons and pions with known fractions of particles of each type. We obtain tagged samples of kaons and pions using data samples of $\phi \to K^+ K^-$ or $D^{*+} \to D^0 \pi^+$ events, with the D^0 decaying to either $K^- \pi^+$ or $K^- \pi^+ \pi^- \pi^+$. The δ_k distributions of kaons and pions are added in proportions ranging from 1:1 to 1:25, and the signal extraction procedure applied. The number of fitted kaons is compared to the true number of input kaons and a ratio ($N_{\mathrm{fit}}/N_{\mathrm{true}}$) determined. The results of this procedure are used to estimate the systematic errors inherent in the signal extraction procedure. We then extrapolate the results of this cross check to the mixture appropriate to each specific decay mode and assess the corresponding systematic error of the signal extraction. The expected fractions of kaons in the measured decay modes, averaged over the momentum range $p > 1.5$ GeV/c, are 1:22, 1:31, 1:49, and 1:34 for the $\tau \to Kh\pi\nu$, $Kh\pi\pi^0\nu$, $KK\pi\nu$, and $KK\pi\pi^0\nu$ analyses, respectively.

The MC modeling error listed in Table III includes the uncertainty in fitting the extracted pion and kaon momentum spectra (i.e., extrapolating into the $p < 1.5$ GeV/c region), as well as the efficiencies for Monte Carlo events to pass both our event and track selection criteria. To evaluate this error, a variety of decay models, both resonant and nonresonant, are used to determine the possible shapes of the dN/dp spectra and to recalculate branching ratios. The following models were investigated in order to evaluate the systematic error for $\tau^- \to K^- \pi^+ \pi^- \nu_\tau$: $\tau \to K_1(1270)\nu_\tau$, $\tau \to K_1(1400)\nu_\tau$, and phase space; for $\tau^- \to K^- K^+ \pi^- \nu_\tau$: $\tau \to K^{*0}K\nu_\tau$, $\tau \to \rho(1690)\nu_\tau$ [$\rho(1690) \to K^{*0}K$], and phase space; for $\tau^- \to K^- \pi^+ \pi^+ \pi^0 \nu_\tau$: $\tau \to K\omega\nu_\tau$ and phase space; for τ^-

$\to K^- K^+ \pi^- \pi^0 \nu_\tau$: $\tau \to K^*K^{*0}$, $\tau \to \rho(1690)\nu_\tau$ [$\rho(1690) \to K^*K^{*0}$], and phase space. To obtain central values, the following primary models were used: the model described in Ref. [11] for the $\tau \to K\pi\pi\nu_\tau$ decay mode [mostly $K_1(1400) \to K^*\pi$]; a mixture of phase space and $\tau \to K\omega\nu_\tau$ in proportions 75:25 for the $\tau \to K\pi\pi\pi^0\nu_\tau$ decay mode; the current KORALB [11] model (including K^*K and ρK) for the $\tau \to KK\pi\nu_\tau$ decay mode; and a mixture of phase space and $\tau \to K^*K^{*0}\nu$ in proportions 50:50 for the $\tau \to KK\pi\pi^0\nu_\tau$ decay mode. Because τ decay modes with kaons are not well understood theoretically, and because data on such decays is sparse, this modeling uncertainty is somewhat large.

To determine the systematic error in our feed-across estimate due to the uncertainty in the input tau decay branching fractions, several different samples of generic τ Monte Carlo were generated using the KORALB package, with branching fractions of the components changed within $\pm 1\sigma$ of the known value. Most feed-across corrections are determined using branching fractions from the Particle Data Group [4]; the magnitude of feed-across corrections internal to this measurement (e.g., $\tau^- \to K^- \pi^+ \pi^- \pi^0 \nu_\tau$ contamination of $\tau^- \to K^- \pi^+ \pi^- \nu_\tau$) are taken from the results of this analysis. The quoted systematic error is derived from the observed variation of the final results when the input branching fractions are varied.

We conservatively assign a 100% systematic error on the hadronic background level (see Table II), since our hadronic simulation may not accurately model the $q\bar{q}$ background. The remaining backgrounds, namely, two-photon events, beam-gas interactions, and QED background, are assessed by varying the event and track selection requirements and determined to be less than 5%. To account for systematics related to photon-finding, and the neutral energy veto, we investigate the dependence of the final results upon the particular values of the cuts used in π^0 reconstruction and the photon

TABLE II. Final results for ratios of branching fractions and derived absolute branching fractions for all four analyses.

Decay mode	Ratio definition	Value ($\times 10^{-2}$)
$\tau \to Kh\pi\nu_\tau$	$\mathcal{B}(\tau \to Kh\pi\nu_\tau)/\mathcal{B}(\tau \to \pi\pi\pi\nu_\tau)$	$5.44\pm0.21\pm0.53$
$\tau \to Kh\pi\pi^0\nu_\tau$	$\mathcal{B}(\tau \to Kh\pi\pi^0\nu_\tau)/\mathcal{B}(\tau \to \pi\pi\pi\pi^0\nu_\tau)$	$2.61\pm0.45\pm0.42$
$\tau \to KK\pi\nu_\tau$	$\mathcal{B}(\tau \to KK\pi\nu_\tau)/\mathcal{B}(\tau \to \pi\pi\pi\nu_\tau)$	$1.60\pm0.15\pm0.30$
$\tau \to KK\pi\pi^0\nu_\tau$	$\mathcal{B}(\tau \to KK\pi\pi^0\nu_\tau)/\mathcal{B}(\tau \to \pi\pi\pi\pi^0\nu_\tau)$	$0.79\pm0.44\pm0.16$

TABLE III. Systematic errors.

Source	Ratio of branching fractions			
	$\dfrac{Kh\pi\nu}{\pi\pi\pi\nu}$	$\dfrac{Kh\pi\pi^0\nu}{\pi\pi\pi\pi^0\nu}$	$\dfrac{KK\pi\nu}{\pi\pi\pi\nu}$	$\dfrac{KK\pi\pi^0\nu}{\pi\pi\pi\pi^0\nu}$
Kaon extraction procedure	6%	7%	9%	8%
MC model uncertainties	2%	6%	9%	15%
τ MC branching fraction uncertainties	2%	9%	4%	3%
MC statistics (for efficiencies)	1%	3%	2%	4%
$q\bar{q}$ background	3%	5%	5%	6%
Other backgrounds (2γ, QED, beam-gas)	5%	5%	5%	5%
Photon finding/veto	4%	6%	10%	6%
Tracking, trigger, tag ID	cancels	cancels	cancels	cancels
Total	10%	16%	19%	20%

veto. This study gives 2–10 % systematic errors (Table III).

We assign a MC statistics error corresponding to the statistical error on the efficiencies and feed-across corrections determined from Monte Carlo simulations. There are other systematic effects that cancel in the final ratio of branching fractions such as trigger efficiencies, tag identification requirements, and track-finding systematics.

VII. SUMMARY

We have measured the following ratios of branching fractions

$$\mathcal{B}(\tau^- \to K^- h^+ \pi^- \nu_\tau)/\mathcal{B}(\tau^- \to \pi^- \pi^+ \pi^- \nu_\tau)$$
$$= (5.44 \pm 0.21 \pm 0.53) \times 10^{-2}, \tag{2}$$

$$\mathcal{B}(\tau^- \to K^- h^+ \pi^- \pi^0 \nu_\tau)/\mathcal{B}(\tau^- \to \pi^- \pi^+ \pi^- \pi^0 \nu_\tau)$$
$$= (2.61 \pm 0.45 \pm 0.42) \times 10^{-2}, \tag{3}$$

$$\mathcal{B}(\tau^- \to K^- K^+ \pi^- \nu_\tau)/\mathcal{B}(\tau^- \to \pi^- \pi^+ \pi^- \nu_\tau)$$
$$= (1.60 \pm 0.15 \pm 0.30) \times 10^{-2}, \tag{4}$$

$$\mathcal{B}(\tau^- \to K^- K^+ \pi^- \pi^0 \nu_\tau)/\mathcal{B}(\tau^- \to \pi^- \pi^+ \pi^- \pi^0 \nu_\tau)$$
$$< 0.0157(95\% \text{ C.L.}), \tag{5}$$

where the limit is quoted because the value in Table II is not statistically significant. Contributions to both denominator and numerator from $\tau \to K_S^0 X$, $K_S^0(\to \pi^+ \pi^-)$ have been excluded. If we instead normalize to $\tau \to h^- h^+ h^- (\pi^0) \nu_\tau$, the corresponding ratio of branching fractions are

$$\mathcal{B}(\tau^- \to K^- h^+ \pi^- \nu_\tau)/\mathcal{B}(\tau^- \to h^- h^+ h^- \nu_\tau)$$
$$= (5.16 \pm 0.20 \pm 0.50) \times 10^{-2}, \tag{6}$$

$$\mathcal{B}(\tau^- \to K^- h^+ \pi^- \pi^0 \nu_\tau)/\mathcal{B}(\tau^- \to h^- h^+ h^- \pi^0 \nu_\tau)$$
$$= (2.54 \pm 0.44 \pm 0.39) \times 10^{-2}, \tag{7}$$

$$\mathcal{B}(\tau^- \to K^- K^+ \pi^- \nu_\tau)/\mathcal{B}(\tau^- \to h^- h^+ h^- \nu_\tau)$$
$$= (1.52 \pm 0.14 \pm 0.29) \times 10^{-2}, \tag{8}$$

$$\mathcal{B}(\tau^- \to K^- K^+ \pi^- \pi^0 \nu_\tau)/\mathcal{B}(\tau^- \to h^- h^+ h^- \pi^0 \nu_\tau) < 0.0154. \tag{9}$$

Subtracting Eq. (8) from Eq. (6) and the central value of Eq. (9) from Eq. (7) we find

$$\mathcal{B}(\tau^- \to K^- \pi^+ \pi^- \nu_\tau)/\mathcal{B}(\tau^- \to h^- h^+ h^- \nu_\tau)$$
$$= (3.64 \pm 0.24 \pm 0.58) \times 10^{-2} \tag{10}$$

and

$$\mathcal{B}(\tau^- \to K^- \pi^+ \pi^- \pi^0 \nu_\tau)/\mathcal{B}(\tau^- \to h^- h^+ h^- \pi^0 \nu_\tau)$$
$$= (1.77 \pm 0.62 \pm 0.42) \times 10^{-2}. \tag{11}$$

Using the CLEO measurements of the decay channels $\tau^- \to h^- h^+ h^- \nu_\tau$ and $\tau^- \to h^- h^+ h^- \pi^0 \nu_\tau$ [12] for the denominator, and Eqs. (8)–(11), we find the branching fractions given in Table IV.

VIII. DISCUSSION

The $\tau^- \to K^- \pi^+ \pi^- \nu_\tau$ decay mode is believed to occur predominantly through coupling to the axial-vector mesons $K_1(1270)$ and $K_1(1400)$. The numerical prediction for the branching fraction of this decay mode calculated by Finkemeier and Mirkes [15] is 0.77%, more than twice as large as both our result as well as the result of ALEPH given in Table IV. Another theoretical prediction, 0.18% by Li [16], is consistent with present measurements.

In contrast to the $K\pi\pi$ mode, tau decays involving the $KK\pi$ final state may occur through either the vector or axial vector currents. Theoretical predictions for the relative amounts of V and A vary considerably [16,20–22]. One can use isospin symmetry to relate the $K^- K^0 \pi^0$, $K^- K^+ \pi^-$, and $K^0 \bar{K}^0 \pi^-$ tau decay modes. The ratio of the branching fractions of these decay modes should be 2:1:1 if $\tau^- \to K^- K^+ \pi^- \nu_\tau$ proceeds exclusively through the $\rho\pi$ inter-

TABLE IV. Recent measurements of $\tau \to K h \pi (\pi^0) \nu_\tau$ decay modes.

τ decay mode	Measurement	Branching fraction, 10^{-2}
$\tau^- \to \bar{K}^0 \pi^- \pi^0 \nu_\tau$	ALEPH [13]	$0.294 \pm 0.073 \pm 0.037$
	CLEO [5]	$0.417 \pm 0.058 \pm 0.044$
$\tau^- \to K^- \pi^+ \pi^- \nu_\tau$	ALEPH [14]	$0.214 \pm 0.037 \pm 0.029$
	This analysis	$0.346 \pm 0.023 \pm 0.056$
	Theory	0.77 [15], 0.18 [16]
$\tau^- \to K^- \pi^0 \pi^0 \nu_\tau$	ALEPH [17]	$0.08 \pm 0.02 \pm 0.02$
	CLEO [18]	$0.14 \pm 0.10 \pm 0.03$
$\tau^- \to K^- K^0 \pi^0 \nu_\tau$	ALEPH [13]	$0.152 \pm 0.076 \pm 0.021$
	CLEO [5]	$0.145 \pm 0.036 \pm 0.020$
$\tau^- \to K^- K^+ \pi^- \nu_\tau$	ALEPH [14]	$0.163 \pm 0.021 \pm 0.017$
	This analysis	$0.145 \pm 0.013 \pm 0.028$
	Theory [15]	0.22
$\tau \to K_S^0 K_L^0 \pi^- \nu_\tau$	ALEPH [13]	$0.101 \pm 0.023 \pm 0.013$
$\tau \to K_S^0 K_S^0 \pi^- \nu_\tau$	CLEO [5]	$0.023 \pm 0.005 \pm 0.003$
	ALEPH [13]	$0.026 \pm 0.010 \pm 0.005$
$\tau \to K^0 \bar{K}^0 \pi^- \nu_\tau$	L3 [19]	$0.31 \pm 0.12 \pm 0.04$
$\tau^- \to K^- \pi^+ \pi^- \pi^0 \nu_\tau$	ALEPH [14]	$0.061 \pm 0.039 \pm 0.018$
	This analysis	$0.075 \pm 0.026 \pm 0.018$
$\tau^- \to K^- K^+ \pi^- \pi^0 \nu_\tau$	ALEPH [14]	$0.075 \pm 0.029 \pm 0.015$
	This analysis	$0.033 \pm 0.018 \pm 0.007$

mediate state or 1:1:1 if this decay proceeds through K^*K. The experimental results for these decay modes are given in Table IV. The decay rate of $\tau \to K^0 \bar{K}^0 \pi^- \nu_\tau$ can be inferred from the ALEPH's measurement for $\mathcal{B}(\tau \to K_S^0 K_L^0 \pi^- \nu_\tau)$ and the combined measurement of CLEO and ALEPH of $\mathcal{B}(\tau \to K_S^0 K_S^0 \pi^- \nu_\tau)$ (Table IV):

$$
\begin{aligned}
& \mathcal{B}(\tau \to K^0 \bar{K}^0 \pi^- \nu_\tau) \\
& = \mathcal{B}(\tau \to K_S^0 K_L^0 \pi^- \nu_\tau) + 2\mathcal{B}(\tau \to K_S^0 K_S^0 \pi^- \nu_\tau) \\
& = (0.149 \pm 0.024 \pm 0.014) \times 10^{-2}.
\end{aligned}
$$

Comparison of these numbers with the isospin-predicted ratios indicates that the bulk of $KK\pi$ production occurs through the vector K^*K intermediate state. This conclusion is consistent with the direct measurement of $\mathcal{B}(\tau \to K^*K\nu_\tau)/\mathcal{B}(\tau \to K^- K^+ \pi^- \nu_\tau) = 0.87 \pm 0.13$ by ALEPH [14].

We can also interpret the available measurements for $\tau \to KK\pi\nu$ to determine the relative couplings of the τ to the strange vector or strange axial vector currents by taking advantage of isospin relations, as in Ref. [23]. If we calculate the ratios

$$
R_v = 1/R_a = \frac{\mathcal{B}_{K^- \bar{K}^0 \pi^0}}{2\mathcal{B}_{K^- K^+ \pi^-} - \mathcal{B}_{K^- \bar{K}^0 \pi^0}}, \quad R = \frac{2\mathcal{B}_{K_S^0 K_S^0 \pi^-}}{\mathcal{B}_{K_S^0 K_L^0 \pi^-}}
\tag{12}
$$

then $R \approx R_v$ indicates vector dominance while $R \approx R_a$ implies axial vector dominance. Combining the available measurements from Table IV we obtain $R = 0.48^{+0.20}_{-0.14}$, $R_v = 0.90^{+0.69}_{-0.37}$, and $R_a = 1.11^{+0.75}_{-0.50}$. The asymmetric errors are defined so that the probability to obtain a measurement within one standard deviation is equal to 68%. Although the values of R, R_a, and R_v favor the vector K^*K state, the results of this method remain inconclusive due to the large errors and the proximity of R_V and R_a to 1. In addition, the value of R, while being closer to R_v, is lower than both R_a and R_v, in contrast to the expectation that R should assume a value between R_a and R_v. If this situation does not resolve itself as errors are reduced, some of the assumptions in the derivation of these relations may have to be reexamined. More precise measurements of the different KK isospin combinations in $\tau \to KK\pi\nu_\tau$ should offer some clarification.

The theoretical prediction for $\mathcal{B}(\tau^- \to K^- K^+ \pi^- \nu_\tau)$ is $\sim 0.2\%$ in Ref. [15]. Our measurement is consistent with this value and the recent ALEPH measurement of this mode [14].

The theory for the τ decays $\tau^- \to K^- \pi^+ \pi^- \pi^0 \nu_\tau$ and $\tau^- \to K^- K^+ \pi^- \pi^0 \nu_\tau$ is more difficult to formulate than that for the three-meson decays discussed above due to the substantially larger number of possible intermediate states. Li [16] has calculated $\tau \to \omega K \nu_\tau = 0.025\%$, which, if correct, would account for approximately 1/3 of our total observed rate for the $\tau^- \to K^- \pi^+ \pi^- \pi^0 \nu_\tau$. Explicit measurements of the substructure in $\tau \to \pi^- \pi^+ \pi^- \pi^0 \nu_\tau$, coupled with these results may help to resolve the nature of these four-meson decays.

ACKNOWLEDGMENTS

APPENDIX: DERIVATION OF RELATIVE RATIO OF BRANCHING FRACTIONS

The expression for the ratio of branching fractions of $\tau \to K h \pi (\pi^0) \nu_\tau$ and $\tau \to \pi \pi \pi (\pi^0) \nu_\tau$ decays is straightforward to derive. Each $\tau \to K h \pi (\pi^0) \nu_\tau$ event contributes one kaon and one pion into the analyzed sample of tracks and

each $\tau \to \pi\pi\pi(\pi^0)\nu_\tau$ contributes two pions. A system of linear equations can be written from which follows the formula

$$\frac{\mathcal{B}[\tau \to Kh\pi(\pi^0)\nu_\tau]}{\mathcal{B}[\tau \to \pi\pi\pi(\pi^0)\nu_\tau]}$$

$$= \frac{N_{Kh\pi(\pi^0)}}{N_{\pi\pi\pi(\pi^0)}} = \frac{N_K^{fit}\phi_{Kh\pi}}{\epsilon_K\phi_{\pi\pi\pi}N_\pi^{fit} - \epsilon_{\pi fk}\phi_{Kh\pi}N_K^{fit}}\frac{2\epsilon_\pi\epsilon_{\pi\pi\pi}}{\epsilon_{Kh\pi}},$$

where N_K^{fit} and N_π^{fit} are the fitted numbers of kaons and pions for a given 1 vs 3 sample, ϵ_K, $\epsilon_{\pi fk}$, and ϵ_π are the efficiencies for a hadron [kaon or pion from $Kh\pi(\pi^0)$ decay or pion from $\pi\pi\pi(\pi^0)$ decay] to pass our track selection requirements, $\epsilon_{Kh\pi}$ and $\epsilon_{\pi\pi\pi}$ are the efficiencies for the indicated

events to pass our 1 vs 3 event selection cuts, and $\phi_{Kh\pi}$ and $\phi_{\pi\pi\pi}$ represent the τ feed-across corrections.

The expression for the decay modes $\tau^- \to K^- K^+ \pi^- \nu_\tau$ and $\tau^- \to K^- K^+ \pi^- \pi^0 \nu_\tau$ is simpler since only one track is taken from each event:

$$\frac{\mathcal{B}[\tau \to KK\pi(\pi^0)\nu_\tau]}{\mathcal{B}[\tau \to \pi\pi\pi(\pi^0)\nu_\tau]} = \frac{N_{KK\pi(\pi^0)}}{N_{\pi\pi\pi(\pi^0)}} = \frac{N_K^{\text{fit}} \cdot \phi_{KK\pi}\epsilon_\pi\epsilon_{\pi\pi\pi}}{N_\pi^{\text{fit}} \cdot \phi_{\pi\pi\pi}\epsilon_K\epsilon_{KK\pi}},$$

where the efficiencies and feed-across corrections have the same meaning as in the previous formula. The values of track efficiencies ϵ_K, $\epsilon_{\pi fk}$, and ϵ_π are $\sim 90\%$ and the event efficiencies $\epsilon_{Kh\pi}$, $\epsilon_{\pi\pi\pi}$ are $\sim 36\%$ for decays without π^0's and $\sim 14\%$ for decays with π^0.

---

[1] Y. S. Tsai, Phys. Rev. D **4**, 2821 (1971).

[2] S. Oneda, Phys. Rev. D **35**, 397 (1987).

[3] T. Das, V. Mathur, and S. Okubo, Phys. Rev. Lett. **18**, 761 (1967).

[4] Particle Data Group, R. M. Barnett *et al.*, Phys. Rev. D **54**, 1 (1996).

[5] CLEO Collaboration, T. Coan *et al.*, Phys. Rev. D **53**, 6037 (1996).

[6] CLEO Collaboration, Y. Kubota *et al.*, Nucl. Instrum. Methods **320**, 66 (1992).

[7] W. P. Elderton and N. L. Johnson, *Systems of Frequency Curves* (Wiley, New York, 1994).

[8] G. J. Hahn and S. S. Shapiro, *Statistical Models in Engineering* (Cambridge University Press, London, 1994).

[9] T. Sjöstrand and M. Bengtsson, JETSET 7.3, Comput. Phys. Commun. **43**, 367 (1987).

[10] R. Brun et al., ''GEANT3 Users Guide,'' Report No. CERN DD/EE/84-1, 1987.

[11] S. Jadach, Z. Was, R. Decker, and J. H. Kühn, Report No. CERN-TH.6793/93.

[12] CLEO Collaboration, R. Balest *et al.*, Phys. Rev. Lett. **75**, 3809 (1995).

[13] ALEPH Collaboration, R. Barate *et al.*, Report No. CERN-PPE/97-167, 1997.

[14] ALEPH Collaboration, R. Barate *et al.*, Report No. CERN-PPE/97-69, 1997.

[15] M. Finkemeier and E. Mirkes, Z. Phys. C **69**, 243 (1996).

[16] B. A. Li, Phys. Rev. D **55**, 1436 (1997).

[17] ALEPH Collaboration, D. Buskulic *et al.*, Report No. CERN-PPE/95-140, 1995.

[18] CLEO Collaboration, M. Battle *et al.*, Phys. Rev. Lett. **73**, 1079 (1994).

[19] L3 Collaboration, M. Acciarri *et al.*, Phys. Lett. B **352**, 487 (1995).

[20] J. J. Gomez-Cadenas, M. C. Gonzalez-Garcia, and A. Pich, Phys. Rev. D **42**, 3093 (1990).

[21] E. Braaten, R. J. Oakes, and S. Tse, Int. J. Mod. Phys. A **5**, 2737 (1990).

[22] R. Decker, E. Mirkes, R. Sauer, and Z. Was, Z. Phys. C **58**, 445 (1993).

[23] A. Rougè, Z. Phys. C **70**, 65 (1996).